Science of the Total Environment 755 (2021) 142602

Contents lists available at ScienceDirect

Science of the Total Environment

journal homepage: www.elsevier.com/locate/scitotenv

Carbon storage and sediment trapping by *Egeria densa* Planch., a globally invasive, freshwater macrophyte

Judith Z. Drexler [a,*], Shruti Khanna [b], Jessica R. Lacy [c]

[a] U.S. Geological Survey, California Water Science Center, 6000 J Street, Placer Hall, Sacramento, CA 95819, USA
[b] California Department of Fish and Wildlife, Bay Delta Region 3, 2109 Arch Airport Road, Suite 100, Stockton, CA 95206, USA
[c] U.S. Geological Survey, Pacific Coastal and Marine Science Center, 2885 Mission St., Santa Cruz, CA 95060, USA

HIGHLIGHTS

- We measured carbon and sediment storage by a globally invasive macrophyte.
- *Egeria densa* stores carbon at rates similar to tidal marshes and seagrasses.
- Carbon and sediment dynamics are likely being altered by *E. densa* worldwide.
- *E. densa* may reduce the ability of tidal marshes to keep pace with sea-level rise.

GRAPHICAL ABSTRACT

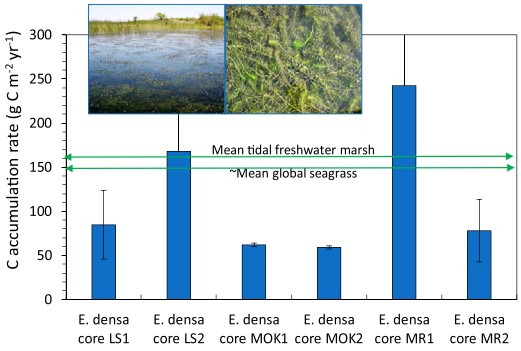

ARTICLE INFO

Article history:
Received 8 April 2020
Received in revised form 15 September 2020
Accepted 19 September 2020
Available online 2 October 2020

Editor: Jan Vymazal

Keywords:
Blue carbon
Carbon sequestration
Ecosystem engineer
Invasive plant
Marsh
Sediment

ABSTRACT

Invasive plants have long been recognized for altering ecosystem properties, but their long-term impacts on ecosystem *processes* remain largely unknown. In this study, we determined the impact of *Egeria densa* Planch, a globally invasive freshwater macrophyte, on sedimentation processes in a large tidal freshwater region. We measured carbon accumulation (CARs) and inorganic sedimentation rates in submerged aquatic vegetation (SAV) dominated by *E. densa* and compared these rates to those of adjacent tidal freshwater marshes. Study sites were chosen along a range of hydrodynamic conditions in the Sacramento-San Joaquin Delta of California, USA, where *E. densa* has been widespread since 1990. Cores were analyzed for bulk density, % inorganic matter, % organic carbon, ^{210}Pb, and ^{137}Cs. Our results show that *E. densa* patches constitute sinks for both "blue carbon" and inorganic sediment. Compared to marshes, *E. densa* patches have greater inorganic sedimentation rates (*E. densa*: 1103–5989 g m^{-2} yr^{-1}, marsh: 393–1001 g m^{-2} yr^{-1}, $p < 0.01$) and vertical accretion rates (*E. densa*: 0.4–1.3 cm yr^{-1}, marsh: 0.3–0.5 cm yr^{-1}, $p < 0.05$), but similar CARs (*E. densa*: 59–242 g C m^{-2} yr^{-1}, marsh: 109–169 g C m^{-2} yr^{-1}, $p > 0.05$). Sediment stored by *E. densa* likely reduces the resilience of adjacent marshes by depleting the sediment available for marsh-building. Because of its harmful traits, *E. densa* is not a suitable candidate for mitigating carbon pollution; however, currently invaded habitats may already contain a meaningful component of regional carbon budgets. Our results strongly suggest that *E. densa* patches are sinks for carbon and inorganic sediment throughout its global range, raising questions about how invasive SAV is altering biogeochemical cycling and sediment dynamics across freshwater ecosystems.

* Corresponding author.
E-mail addresses: jdrexler@usgs.gov (J.Z. Drexler), ShrutiKhanna@Wildlife.ca.gov (S. Khanna), jlacy@usgs.gov (J.R. Lacy).

https://doi.org/10.1016/j.scitotenv.2020.142602

1. Introduction

Invasions by non-native plant species are a major cause of global change, often irreparably altering ecosystem properties and functions in their naturalized habitats (Evangelista et al., 2014; Powell et al., 2011; Santos et al., 2011; Vilá et al., 2009; Vitousek et al., 1996). Freshwater ecosystems have particularly high invasion pressure due to the plethora of sources providing unintentional and intentional releases of non-native species, the multitude of vectors involved in initial dispersal, and the ease with which secondary dispersal occurs across aquatic systems (Lodge et al., 1998; Moorhouse and Macdonald, 2015; Reid et al., 2019). In addition to transforming ecological structure and function, highly invasive, non-native plants also interfere with human enterprises such as electricity generation, navigation, and fishing (Boudouresque et al., 1995; Gallardo et al., 2016; Global Invasive Species Database (GISD), 2019a; Martin et al., 2018; Masifwa et al., 2001). A prime example of such an impactful species is *Egeria densa* Planch., which is recognized by the International Union for the Conservation of Nature as a globally important invader in both temperate and tropical freshwater ecosystems (GISD, 2019b) (Fig. 1).

E. densa is a perennial species of freshwater submerged aquatic vegetation (SAV) native to the central Minas Gerais region of Brazil, coastal Argentina, and coastal Uruguay (Cook and Urmi-König, 1984). It was introduced to North America, Europe and Australia as an ornamental plant predominantly for use in aquariums and decorative ponds (Cook and Urmi-König, 1984; Curt et al., 2010; Gillard et al., 2017; Yarrow et al., 2009). Currently, *E. densa* is found on all continents except Antarctica (Alfasane et al., 2010; Curt et al., 2010; Strange et al., 2018; Yarrow et al., 2009). *E. densa* is a particularly adept competitor due to its abundant growth, overwintering shoots, ability to grow in low light and cool temperatures, and flexible nutrient uptake from the water column and sediment (Curt et al., 2010; Getsinger and Dillon, 1984; Santos et al., 2011). Furthermore, *E. densa* displays high phenotypic plasticity, broad dispersal through vegetative fragments, and a great capacity to colonize disturbed areas (Santos et al., 2011; Yarrow et al., 2009).

In addition to its ability to quickly expand its range, *E. densa* acts as an autogenic ecosystem engineer (*c.f.*, Jones et al., 1994a, 1994b) by transforming ecosystem properties and functions through its physical structure (Yarrow et al., 2009). Its aggressive growth and alteration of temperature, oxygen, and nutrient levels have been associated with the loss of native SAV communities, reduction in phytoplankton productivity, and expansion of predatory invasive fish habitat (Brown, 2003; Conrad et al., 2016; Durand et al., 2016; Nobriga and Feyrer, 2007; Simenstad et al., 1999). *E. densa* also changes physical aspects of freshwater ecosystems by reducing water velocity and increasing channel incision (Champion and Tanner, 2000; Wilcock et al., 1999).

Some aspects of *E. densa's* ecosystem engineering capabilities are less well understood. Several studies have hypothesized that by slowing flows, *E. densa* increases inorganic sediment deposition on the channel bed or lakebed (Champion and Tanner, 2000; Hestir et al., 2016; Yarrow et al., 2009). This ability to trap sediment has been well demonstrated for both marine and freshwater species of SAV (Madsen et al., 2001; Sand-Jensen, 1998). For freshwater SAV, however, few measurements exist for the *rates* of such sediment deposition. A recent study by Work et al. (2020) provides measurements of instantaneous sediment trapping in channel environments and demonstrates that ~5% of incident sediment is deposited in patches of *E. densa*. However, due to a lack of direct measurements of vertical accretion and inorganic sedimentation rates, it is unknown whether or not *E. densa* patches act as long-term sediment sinks on the landscape. In addition, recent work has shown that *E. densa* can increase concentrations of dissolved inorganic carbon and dissolved inorganic nitrogen in the lower water column and augment gaseous fluxes of both carbon dioxide and methane to the atmosphere (Ribaudo et al., 2014; Ribaudo et al., 2018). Despite this work, the full impact of *E. densa* on carbon cycling, including whether or not it provides the highly valuable ecosystem service of carbon storage, is largely unknown.

In recent years, seagrasses, which are marine SAV, have been recognized together with salt marshes and mangroves as accumulating and storing high amounts of organic carbon, termed coastal "blue carbon", in addition to inorganic matter in their sediments (Lavery et al., 2013; McLeod et al., 2011; Nellemann et al., 2009; Windham-Myers et al., 2019). Just recently, carbon stocks have been determined for estuarine SAV along a salinity gradient from saline to fresh (Hillman et al., 2020), but to date there are still no direct measurements of carbon accumulation rates (CARs) in freshwater SAV. The greater invasive plant literature also lacks data on CARs. Although studies have shown that several terrestrial and aquatic species increase belowground carbon content of soils and sediment (Davidson et al., 2018; Liao et al., 2008 and reference therein; Vilá et al., 2011), such research focuses almost entirely on static properties such as organic carbon stocks rather than direct measurements of CARs over time.

Ecosystem processes such as CARs and inorganic sedimentation rates are critical for understanding the long-term impacts of invasive species, because these processes act on scales of decades or longer. *E. densa* is a particularly apt species for studying these processes because it is so broadly distributed around the world and across freshwater ecosystem types and has an invasion history of over half a century in many areas (Light et al., 2005; Yarrow et al., 2009). If invasive SAV such as *E. densa* were to function as a sink for both inorganic sediment and organic carbon, this would represent a rare example of how chronic plant invasion can simultaneously alter both sediment dynamics and biogeochemical cycling on an ecosystem scale.

In this study, we measured the impact of invasive SAV dominated by *E. densa* on carbon accumulation and inorganic sedimentation in the Sacramento-San Joaquin Delta of California, USA, which is a 2400 km^2 region at the landward end of the San Francisco Estuary (hereafter, the Delta, Fig. 2). This predominantly freshwater region, which is within the tidal zone of the estuary, provides a surfeit of suitable study sites due to its large size, wide range of hydrodynamics, and ~3000 ha of *E. densa*-dominated infestation. Overall, the main questions we sought to answer were (1) are *E. densa* patches sinks for blue carbon and inorganic sediment on the landscape? and (2) how do CARs compare among *E. densa* patches, adjacent tidal freshwater marshes, and other blue carbon ecosystems around the world? We selected three study sites with differing hydrodynamics because research in both tidal marshes (Adame et al., 2010; Drexler et al., 2009; Hatton et al., 1983) and SAV (Ganthy et al., 2015; van Katwijk et al., 2010) has shown that sediment trapping is influenced by the level of hydrodynamic energy. At each site, we collected cores in tidal freshwater marshes and adjacent patches of *E. densa* in order to compare and contrast the inorganic sedimentation rates and CARs in each of these settings.

2. Materials and methods

2.1. Study sites

The Delta is part of a 163,000 km^2 watershed, bounded by the Sierra Nevada and Cascade Ranges of California (Cloern et al., 2011). Before European settlement, it was dominated by tidal freshwater marshes, which began forming approximately 6800 years ago (Drexler et al., 2009; Drexler, 2011). The Delta region receives runoff from more than 40% of the land area of California and discharges to the Pacific Ocean through northern San Francisco Bay (California Department of Water Resources, 1995) (Fig. 2). Tides in the estuary are mixed semidiurnal and micro-tidal, and tidal range is approximately 1 m from mean lower low water to mean higher high water (Atwater, 1980; Conomos et al., 1985; Shlemon and Begg, 1975). The climate of the region is characterized as Mediterranean with cool winters and hot, dry summers (Atwater, 1980). Mean annual precipitation is approximately 36 cm, but yearly precipitation can vary from half to almost four times this amount. More than 80% of precipitation occurs from November to March and most freshwater inflow to the Delta occurs from January to

Fig. 1. Close-up of *E. densa* at the water surface and a view of its infestation in the Sacramento-San Joaquin Delta of California (credit: Center for Spatial Technologies and Remote Sensing, University of California, Davis, inset 2006, landscape 2019).

June because of storage in the snowpack and releases from reservoirs (Knowles, 2002). Beginning in the mid-1800s, the Delta was almost entirely drained for agriculture (Atwater, 1980; Thompson, 1957), resulting in its current configuration of more than 100 islands and tracts surrounded by 2250 km of man-made levees and 1130 km of waterways (Prokopovich, 1985) (Fig. 2).

Delta marshes are dominated by emergent macrophytes and scrub-shrub wetland species. Major macrophytes include *Schoenoplectus californicus* (C.A. Mey.) Soják (Californian bulrush), *Typha* spp. (cattails), and *S. acutus* (Muhl. ex Bigelow) Á. Löve and D. Löve (hardstem bulrush) and major tree/shrub species include *Cornus sericea* L. (red osier dogwood) and *Salix lasiolepis* Benth. (arroyo willow). SAV in the Delta consists mainly of *E. densa* (invasive), *Myriophyllum spicatum* L. (watermilfoil, invasive), *Potamogeton nodosus* Poir. (longleaf pondweed, native), *Potamogeton crispus* L. (curly leaf pondweed, invasive), *Stuckenia pectinata* (L.) Börner (Sago pondweed, native), *Cabomba caroliniana* A. Gray (Carolina fanwort, invasive), *Ceratophyllum demersum* L. (coontail, native), and *Elodea canadensis* Michx. (Canadian waterweed, native) (Khanna et al., 2018). Botanical nomenclature follows Jepson Flora Project (2020) and U.S. Department of Agriculture, Natural Resources Conservation Service (2020). Marsh soils in the Delta consist mainly of highly organic "peat" soils (histosols) replete with robust *Schoenoplectus* roots (Drexler et al., 2019), while channel bed sediments consist almost entirely of inorganic sediment (Schoellhamer et al., 2012).

In California, *E. densa* is found in freshwater ecosystems along the coast, in the Central Valley, as well as in the Sierra Nevada (U.S. Geological Survey, 2019). In the Delta, *E. densa* is the most aggressive and common species of invasive SAV (Boyer and Sutula, 2015; Santos et al., 2012). *E. densa* first arrived in the Delta in 1946 (Light et al., 2005) and by 1990 it was widespread across the region, spurring the state legislature to authorize the development of a control program in 1996 (USDAARS-CDBW, 2012). Focused treatments of *E. densa* in the Delta began in 2001, but the infestation continued to spread. Cover of invasive SAV increased from 2080 ha in June 2008 to 4970 ha in 2015 with *E. densa* accounting for 60–66% of the total area covered by SAV (Ustin et al., 2015). The percent cover of Delta waterways by invasive SAV increased from only 8.4% in 2008 to a peak of 36% in 2017 (Ustin et al., 2019). Invasive SAV is found predominantly in shallow areas of channels, particularly along the channel edge.

We chose three study sites that represented a range of hydrodynamic conditions and sediment availability (Fig. 3). Lindsey Slough (LS), located in the northwest of the Delta within the Cache Slough Complex, is a relatively turbid tidal backwater of the Sacramento River (Morgan-King and Schoellhamer, 2013). LS is a dead-end slough and, as a result, it receives little runoff. Currents at LS are dominated by tides and are relatively weak. We focused on a marsh island (1.7 ha) and surrounding patches of SAV in the southeastern part of the slough (Fig. 3). The second site, the lower Mokelumne (MOK), is situated in the central Delta at the confluence of the Mokelumne River and the San Joaquin River. MOK directly receives runoff and sediment from the 1700 km^2 watershed of the Mokelumne River (Ahearn et al., 2005) and exhibits the strongest currents and greatest riverine influence of the three sites. At the lower Mokelumne River (USGS gage 11325500), maximum annual mean flow is 61 $m^3\ s^{-1}$ (U.S. Geological Survey, 2020) and during high discharge events, flow can be directed downstream throughout the entire tidal cycle. At MOK we focused on a 1.21 ha marsh island (Fig. 2). The third site is situated in Middle River (MR) in the southern Delta. Currents at MR are predominately tidal, but are somewhat stronger than at LS. MR is influenced by San Joaquin River flows and the cross-Delta transport of water to export pumps, which direct water to the south. Suspended sediment concentrations are typically very low in this region of the Delta. We focused on a 20.3 ha marsh island in the southwest part of Middle River for the study (Fig. 3). At all three study sites, SAV patches dominated by *E. densa* were found within 5 m of the marsh edge.

2.2. Core collection

Push cores were collected with 1.5 in. (3.8 cm) interior diameter plexiglass tubing in April and October 2017 at LS and in March 2018 at MR and MOK. Within SAV patches, the tubing was pushed by hand directly into the sediment bed from a small vessel. Outside the SAV, where the water was too deep to collect push cores directly from the vessel, Gomex box cores (0.0625 m^2) were collected and subsampled with push cores. Push cores were stored vertically, kept on ice, and transported to the U.S. Geological Survey (USGS) laboratory in Santa Cruz, CA.

Long cores in SAV (*E. densa*) at all three sites were collected in April 2018 from a pontoon boat platform moored over SAV patches adjacent to the marsh islands. Cores were collected with a gravity corer to ~60–80 cm in depth in 3.25 in. (8.35 cm) interior diameter cellulose tubing. SAV cores were sectioned in the field into 2-cm sections shortly after collection. Core sections were placed in labeled plastic bags and transported on ice to the USGS laboratories in Sacramento, CA.

During May 2018, two long (~50 cm) peat cores were collected in each marsh ~5 m from the marsh edge. Cores were collected with a Hargis corer, a razor-edged, piston corer (15 cm diameter), which minimizes soil compaction (Hargis and Twilley, 1994). After collection, cores were sealed airtight on both ends within their acrylic collection tubes, laid horizontally on ice, and transported to the USGS laboratories in Sacramento for further processing.

2.3. Core analysis

All push cores were divided into 1 cm vertical sections within 24 h of collection and stored in pre-weighed whirl-pak bags. The samples were weighed wet, dried at 60 °C, and weighed again. Drying continued until weights stabilized. The dry bulk density (BD) of the push cores reported here was calculated as: $BD = (1-P)\rho_s$, where porosity P is the fraction of water by volume, and sediment density ρ_s is 2.65 g cm^{-3}.

In the laboratory, peat cores from the marsh sites were sectioned into 2 cm sections. Both SAV and peat core sections were weighed wet, dried at 60 °C, and weighed again. Bulk density was determined on both SAV and peat cores by dividing the dry weight of each 2 cm peat section by the volume of the section. All peat and SAV core sections were then ground to pass through a 2 mm sieve.

Total percent organic carbon on all core samples was measured using a Perkin Elmer CHNS/O elemental analyzer (Perkin Elmer

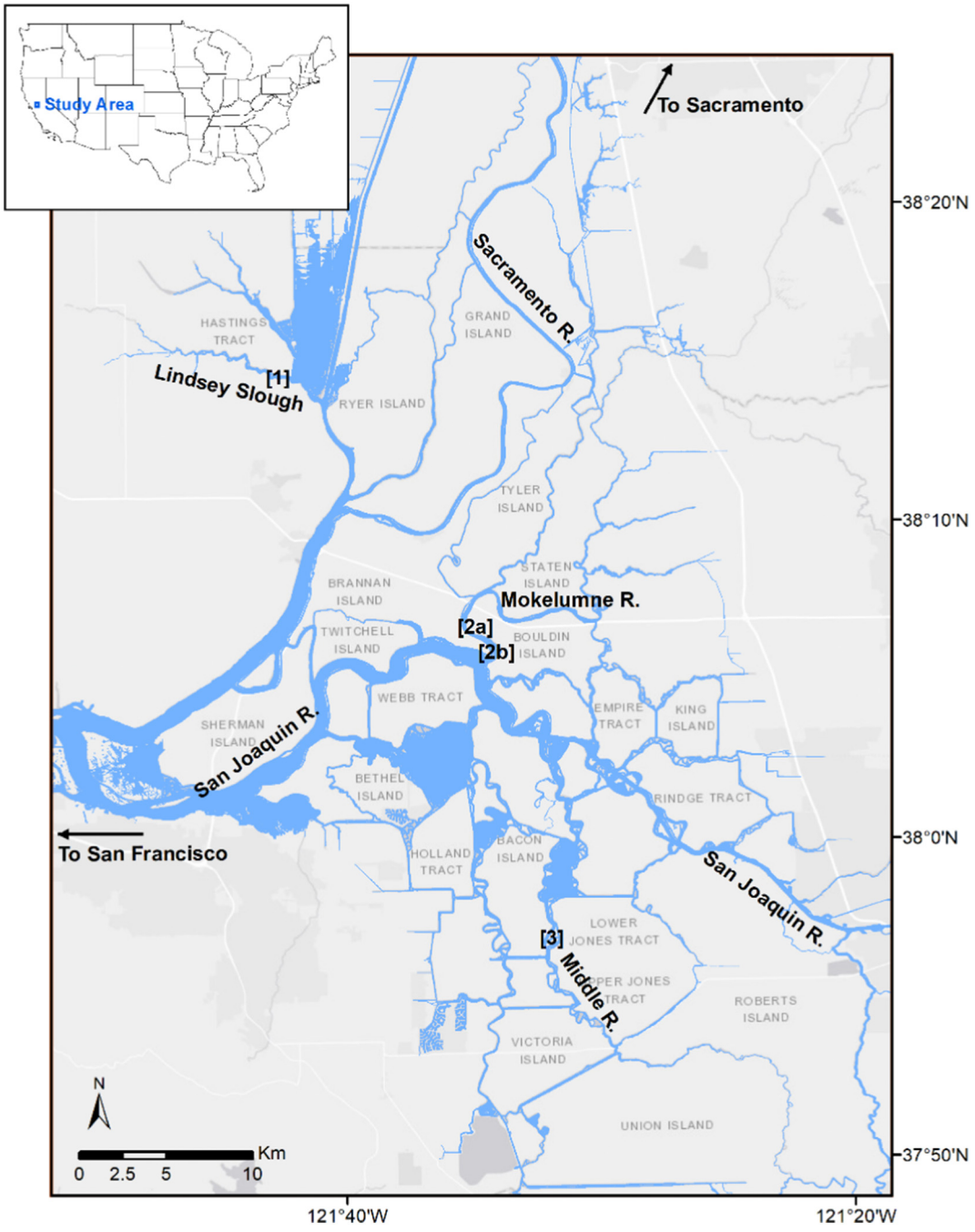

Fig. 2. Map showing the location of the Sacramento-San Joaquin Delta in California, USA and the three study sites, Lindsey Slough, Mokelumne River, and Middle River, within the Delta region.

Corporation, Waltham, Massachusetts, USA) following a modified version of U.S. Environmental Protection Agency Method 440.0 (Zimmerman et al., 2007). Samples were first exposed to concentrated hydrochloric acid fumes in a desiccator for 24 h to remove inorganic carbon, which was a minor percentage of carbon content. The elemental analyzer was calibrated with blanks and acetanilide standards before use. Every ten samples, blanks, replicates, and standards were analyzed to check for instrument stability. If the percentage difference between the two replicates was greater than 20%, replicate samples were reanalyzed. The detection limit for carbon was 0.01% by weight.

Mud (silt and clay fractions <63 μm), sand (63 μm–2 mm), and gravel (>2 mm) fractions on sections of push cores, SAV cores, and peat cores were determined in the USGS laboratory in Santa Cruz, CA. Approximately 20 g of sediment was sub-sampled and 10 mL of 35% hydrogen peroxide was added to remove organic material in the sample. The sample was heated to 250 °C to remove any remaining hydrogen peroxide and was placed in an ultrasonic bath to liberate the fine fraction. Subsequently, the sample was centrifuged for 1.5 h to remove soluble salts. Samples were funneled through a 2 mm and a 63 um sieve to separate the gravel, sand, and mud. The sand and gravel fractions were dried in an 80 °C oven and weighed. Five mL of sodium hexametaphosphate was added to the mud fraction and a 20 mL aliquot was taken from a 1 L graduated cylinder to determine the weight of the mud.

Subsections of marsh cores and SAV cores were analyzed at the USGS in Menlo Park, California, for ^{137}Cs, ^{210}Pb, and ^{226}Ra. Activities of total ^{210}Pb, ^{226}Ra, and ^{137}Cs were measured simultaneously by gamma spectrometry as described in Drexler et al. (2017). Radioisotope activities of subsections were measured using a high-resolution intrinsic

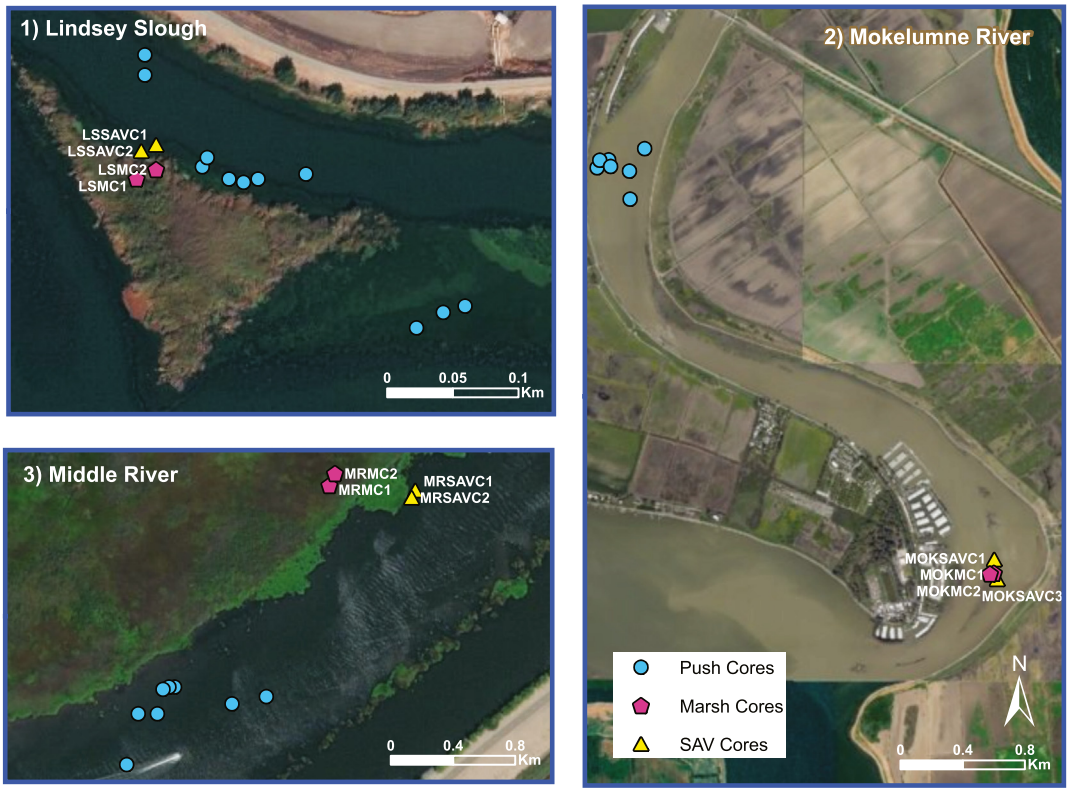

Fig. 3. Images of the three study sites, Lindsey Slough (LS), Mokelumne River (MOK), and Middle River (MR), showing submerged aquatic vegetation (SAV) dominated by *E. densa* in red and emergent marsh in green (dark green = healthy emergent vegetation, lighter green = senescent emergent vegetation). Sites are numbered in accordance with Fig. 2. SAV and marsh cores are labeled with site abbreviation first, SAVC (SAV core) or MC (marsh core) next, and core number last. SAV coverage maps were created using AVIRIS-NG 2.5 × 2.5 m 432 band imagery collected in Fall of 2015 (for the entire Delta including Middle River) and HyMap 1.7 × 1.7 m 126 band imagery collected in Fall of 2018 (for Mokelumne River and Lindsey Slough) (Ustin et al., 2016, 2019; Khanna et al., 2018). Service layer source credits: Esri, DigitalGlobe.

germanium well detector gamma spectrometer. Samples were measured in the detector borehole, which provides near 4π counting geometry. Samples were all sealed in 7 mL polyethylene scintillation vials. The supported ^{210}Pb activity, which is defined by the ^{226}Ra activity, was determined on each core section from the 352 keV and 609 keV gamma emission lines of the short-lived daughters ^{214}Pb and ^{214}Bi daughters of ^{226}Ra, respectively. The activity of ^{137}Cs was determined from the 661.5 KeV gamma emission line. Self-absorption of the ^{210}Pb 46 keV gamma emission line was determined and accounted for using an attenuation factor calculated from an empirical relationship between self-absorption and bulk density based on the method of Cutshall et al. (1983). Additional information regarding quality assurance/quality control can be found in Drexler et al. (2017).

Marsh cores and SAV cores were dated using both ^{210}Pb and ^{137}Cs. For ^{210}Pb dating, the decay of the excess ^{210}Pb vs. cumulative dry mass was used (constant flux: constant sedimentation rate approach) to estimate a mean vertical accretion rate for each core (Appleby and Oldfield, 1983; Drexler et al., 2017). The constant rate of supply model, which provides a unique accretion estimate for each section of a core, could not be used because the entire profile of excess ^{210}Pb was not recovered in the core profiles. Due to low activities of ^{137}Cs on the west coast of the U.S. and the possibility of mobility in the peat column (Drexler et al., 2018), we used ^{210}Pb exclusively for dating *unless* the only estimates available were from ^{137}Cs. ^{210}Pb values in the top 30 cm of cores were used to date core profiles because this depth range yielded the best results using the constant flux: constant sedimentation approach. CARs were determined by multiplying the vertical accretion rate by the mean carbon density. Inorganic sedimentation rates were determined by multiplying the vertical accretion rate by the mean inorganic matter density. Uncertainties in ^{210}Pb dating were estimated following the method of Van Metre and Fuller (2009). Uncertainties for ^{210}Pb dates were propagated into estimates of vertical accretion using the following expression: VA $*$ (sd_{MAR})/MAR where MAR is the mass accumulation rate of all material in g cm^{-2} yr^{-1}, and sd_{MAR} is the standard deviation of the MAR. Uncertainties in CARs and inorganic sedimentation rates were estimated by multiplying the ^{210}Pb-derived vertical accretion rate by the mean carbon density and mean inorganic matter density, respectively. Because including the top 30 cm layer of cores was required for best dating results, it is likely that some underlying bed sediments formed prior to *E. densa* infestation were also included in the 30 cm, leading to potential underestimation of these rates in patches of *E. densa*.

^{137}Cs dating was only carried out if distinct ^{137}Cs peaks were found along the core profile. Vertical accretion rates were calculated by dividing the depth of the ^{137}Cs peak by the time period, x, between the date of core collection date and 1963 (x = 55 years for this study). CARs and inorganic sedimentation rates were estimated using the ^{137}Cs-derived vertical accretion rate and the mean carbon and inorganic matter densities as described above. Uncertainties in ^{137}Cs dating were estimated according to the approach of Drexler et al. (2017), which likely underestimates total uncertainty because this method only considers potential error in the position of the 1963 peak and cannot quantify uncertainty related to the possible migration of ^{137}Cs in situ. Uncertainties in carbon accumulation and inorganic sedimentation rates were estimated by multiplying the uncertainty in the ^{137}Cs-derived vertical accretion rate by the mean carbon density and mean inorganic matter density, respectively. Because the ^{137}Cs dating method relies on the 1963 peak and this dating horizon occurred before broad infestation in 1990, it is likely that we underestimate CARs and inorganic sedimentation rates in *E. densa* patches.

2.4. Statistical analysis

For this study, all statistical analyses were carried out using SYSTAT 13.00.05. Bulk density, % organic carbon, and % mud from the top cm of the push cores were compared between the unvegetated channel and the channel bed under SAV to determine whether basic properties of sediments differ between these two environments. All coring sites were compared collectively using two-tailed Student's *t*-tests and an alpha level of 0.05. In addition, in order to determine any differences in % OC and % mud in push cores across sites, one-way ANOVA was carried out with site as the factor with an alpha level of 0.05. The Shapiro-Wilk test was used to check normality of data and Levene's test was used to check homogeneity of variances. Percent OC data were log-transformed prior to ANOVA to meet test assumptions. Post-hoc pairwise comparisons were done using Tukey's Honestly Significant Difference test with an alpha level of 0.05.

Two-way ANOVA was used to test the influence of site and core type on mean bulk density and % organic carbon in the top 30 cm of long cores collected in marshes and SAV. For each test, an alpha level of 0.05 was used, normality of data was checked using the Shapiro-Wilk test, and homogeneity of variances was checked with Levene's test. Post-hoc pairwise comparisons were done as stated above.

Mean inorganic sedimentation rates and mean CARs were compared between marsh and SAV cores using two-tailed Students t-tests with an alpha level of 0.05.

3. Results

Basic properties of sediments in the unvegetated channel differed significantly from those under *E. densa* (indicated as "SAV" in figures and tables). The bulk density of the top cm of push cores collected at MOK, LS, and MR (Supplementary Information: Table A1) was significantly greater in the unvegetated channel than under SAV (Student's t-test, $p < 0.0001$). The biggest difference between bulk density in SAV and the unvegetated channel was found at MOK (Fig. 4). Percent organic carbon in the top cm of push cores (Table A1) was significantly greater under SAV than in the unvegetated channel (Student's t-test, $p < 0.0001$).

There was a significant difference in % organic carbon of push cores between the sites (Table 1). Mean % organic carbon under SAV was greater at each individual site than in the unvegetated channel (Fig. 4). Post-hoc pairwise comparisons showed that % organic carbon under SAV at LS and MOK did not significantly differ ($p > 0.05$), but that both were less than at MR ($p < 0.001$). In the unvegetated channel, post-hoc pairwise comparisons showed that % organic carbon differed between the sites with LS > MR > MOK (p values <0.001).

The fine sediment fraction (% mud) in push cores differed between sites, illustrating how both hydrodynamics and SAV influence particle size (Table 1, Fig. 4). At LS, which is the most quiescent site, mud comprised almost the entire top cm in both SAV and the unvegetated channel (Fig. 4; Table A1). At MR, mud comprised almost the entire top cm in the SAV but made up less than 20% in the unvegetated channel (Fig. 4). At MOK, the mean % mud was still high in the SAV (88.7 ± 13.3%), but very low in the unvegetated channel (2.6 ± 1.2%) (Fig. 4, Table A1). These low values for fines in the unvegetated channel at MR and especially MOK indicate higher energy conditions at these sites relative to LS. The higher % fines in SAV in comparison to the unvegetated channel reflect the reduction of current speed within SAV patches, which results in the settling of fine particles. Post-hoc pairwise comparisons showed % mud in the top cm of the unvegetated channel at LS > MR > MOK (p values <0.001, Fig. 4). In the SAV, post-hoc pairwise comparisons showed that % mud at LS ($p = 0.003$) and MR ($p = 0.024$) was greater than at MOK; however no significant difference was found between LS and MR ($p = 0.954$).

For long cores collected in SAV patches and marshes, a two-way ANOVA of bulk density with sites and core type as factors was

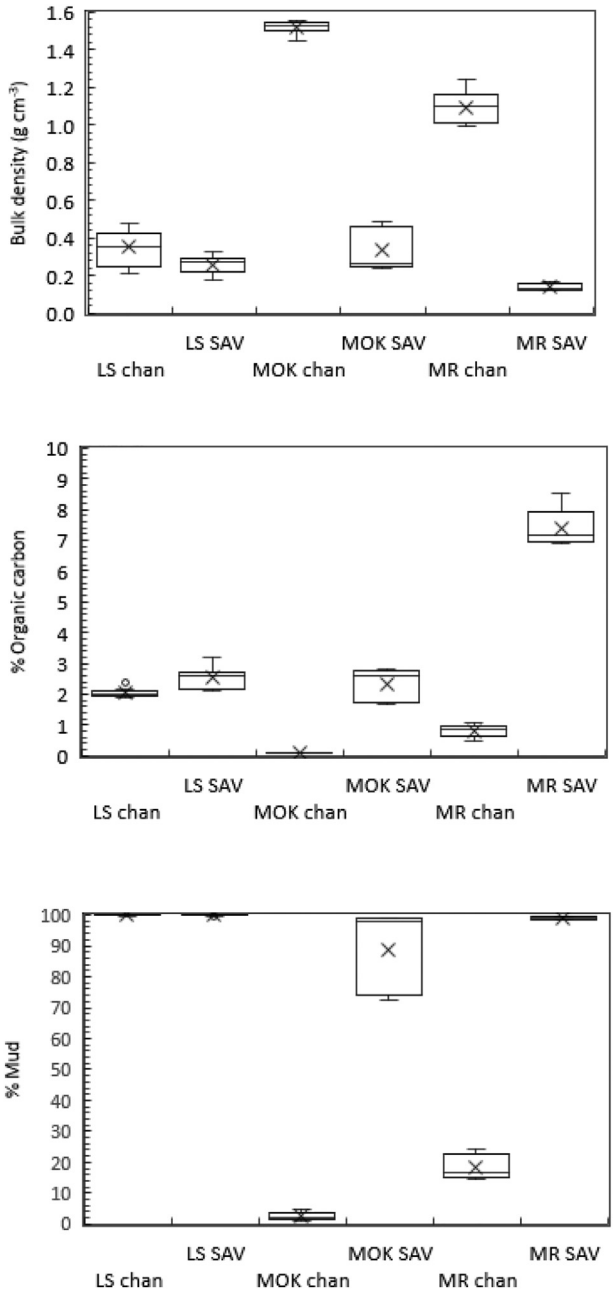

Fig. 4. Box plots of bulk density, % organic carbon, and % mud for the top cm of push cores from the unvegetated channel (chan) and SAV (*E. densa*) at LS, MOK, and MR. In each box, an "x" marks the mean and a horizontal line marks the median. Box length indicates the range within which the central 50% of the values fall, with the box edges or hinges at the first and third quartiles. Whiskers show the range of observed values that fall within the inner fences (lower inner fence = lower hinge − (1.5 * Hspread); upper inner fence = upper hinge + (1.5 * Hspread) where Hspread is the interquartile range).

significant for both factors (Fig. 5a, Table 2, Supplementary Information: Table A2). Post-hoc pairwise comparisons showed that MOK has higher bulk density than both LS ($p = 0.003$) and MR ($p < 0.001$), which have no significant difference between them ($p = 0.076$). A post-hoc pairwise comparison also showed that SAV cores have higher bulk density than marsh cores ($p = 0.001$). The interaction term between sites and core type was not significant (Table 2, Supplementary Information: Fig. A1).

For long cores, a two-way ANOVA of % organic carbon with sites and core type as factors was significant for both factors (Fig. 5b, Table 3, Table A2). Post-hoc pairwise comparisons showed that % organic carbon

Table 1
One-way ANOVA results for % organic carbon and % mud data from push cores collected in both the unvegetated channels and under SAV (*E. densa*) at each of the three sites.

% OC in the unvegetated channel:	Type III SS	Degrees of freedom	Mean Squares	F-ratio	p-value
Sites	60.383	2	30.192	909.952	<0.001
Error	1.062	32	0.033		
% OC in SAV:					
Sites	4.847	2	2.424	102.868	< 0.001
Error	0.518	22	0.024		
% Mud in unvegetated channels:					
Sites	71,120.503	2	35,560.251	8,213.020	<0.001
Error	138.552	32	4.330		
% Mud in SAV:					
Sites	476.706	2	238.353	7.424	0.003
Error	706.324	22	32.106		

at MR > LS > MOK (p values ≤0.05) and that marsh cores have greater % organic carbon than SAV cores ($p < 0.001$). The interaction term was significant (Table 3, Supplementary Information: Fig. A1), indicating

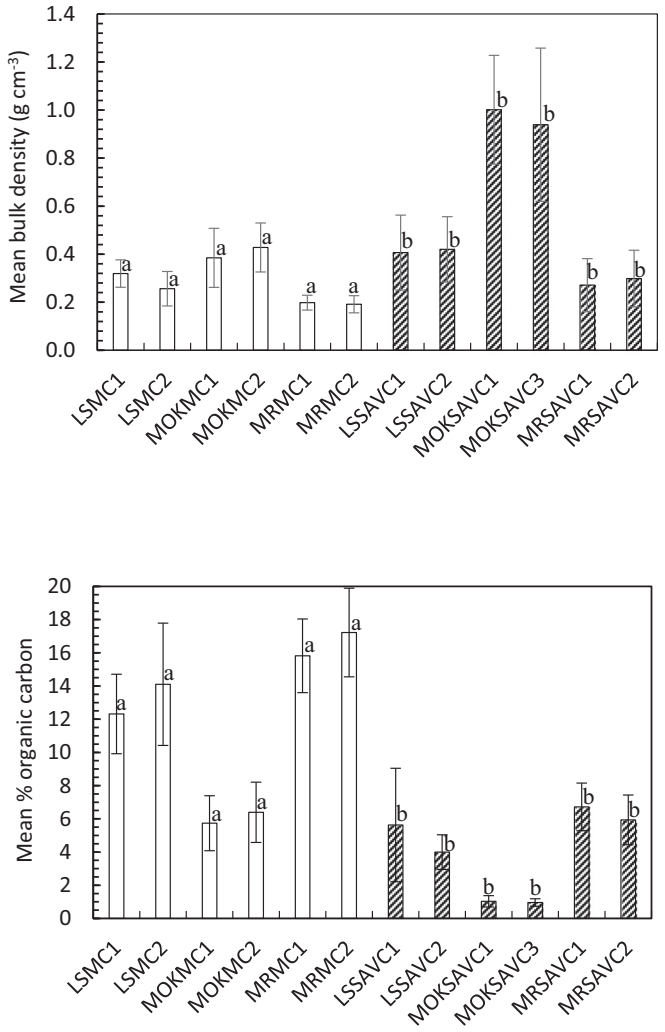

Fig. 5. Plots of (a) mean bulk density and (b) mean % organic carbon content in the top 30 cm of cores. Cores are labeled by site (LS, MOK, and MR), type (MC = marsh core; SAVC = SAV core), and number (1 or 2). Different letters (a vs. b) show statistically significant differences between SAV and marsh cores at $p < 0.05$.

Table 2
Two-way ANOVA of bulk density with sites and core type (marsh vs. SAV) as factors.

Source	Type III SS	Df	Mean Squares	F-ratio	p-value
Sites	0.391	2	0.195	38.122	<0.001
Core type	0.177	1	0.177	34.607	0.001
Site * Core type	0.044	2	0.022	4.320	0.069
Error	0.031	6	0.005		

that the effect of site and core type was not simply additive. The lower % organic carbon at MOK likely stems from the fact that it is a much higher energy site than either LS and MR due to its main stem location and, because of this, SAV and marshes at MOK receive a greater amount of inorganic sediment (see below). This translates into less % organic carbon per unit volume at MOK than at LS and MR. The significant interaction term shows that, in addition to the low % organic carbon in the SAV and marshes at MOK, the enrichment of % organic carbon in marsh relative to SAV is also less at MOK than the other sites (Fig. 5). We attribute both effects (site and interaction) to the relatively high sediment availability at MOK.

All cores were dated with ^{210}Pb except MOKSAVC1 and MOKSACV3, which were determined with ^{137}Cs because dating was not possible with ^{210}Pb. Two cores, MOKMC1 and MOKMC2, could not be dated due to erroneous values of both ^{210}Pb and ^{137}Cs (Supplementary Information: Table A3). Low fallout rates in the western United States combined with dynamic local conditions, such as the high energy environment at MOK, created challenges for dating sediments with ^{137}Cs and ^{210}Pb (Drexler et al., 2017, 2018). Without proper dating, the vertical accretion rates, CARs, and inorganic sedimentation rates could not be determined for MOKMC1 and MOKMC2.

Vertical accretion rates ranged from 0.3 to 0.5 cm yr^{-1} for marsh cores and from 0.4 to 1.3 cm yr^{-1} for SAV cores for the top 30 cm of each core (Fig. 6, Table A4). In SAV cores, vertical accretion rates were significantly greater and also more variable than in marsh cores, likely due to the dynamic conditions in channel environments, which can result in greater accumulation but also greater erosion than in marshes (Students one-tailed *t*-test, $p < 0.05$).

Mean inorganic sedimentation rates within the top 30 cm ranged from 393 to 1001 g sediment m^{-2} yr^{-1} in marsh cores and 1103 to 5989 g sediment m^{-2} yr^{-1} in SAV cores (Fig. 7). Mean inorganic sedimentation rates were significantly greater in SAV cores than marsh cores (Students t-test, $p < 0.01$).

Mean CARs over the datable period (top ~30 cm) ranged from 109 to 169 g C m^{-2} yr^{-1} for marsh cores and 59–242 g C m^{-2} yr^{-1} for SAV cores (Fig. 7). CARs were not significantly different between marsh cores and SAV cores (Students t-test, $p > 0.05$).

Using the total area dominated by *E. densa* in the Delta (~3000 ha; Ustin et al., 2015) and the mean CAR and inorganic sedimentation rates in patches shown above (116 ± 75 g C m^{-2} yr^{-1} and 3466 ± 748 g sediment m^{-2} yr^{-1}, respectively), we estimate total carbon and inorganic sediment storage in *E. densa* patches in the Delta to be ~3500 ± 2200 metric tons C yr^{-1} and ~103,000 ± 22,000 metric tons inorganic sediment yr^{-1}, respectively.

4. Discussion

Here we show for the first time that *E. densa*, a species of invasive SAV, is transforming aquatic ecosystems by acting as a long-term sink

Table 3
Two-way ANOVA of % organic carbon with sites and core type (marsh vs. SAV) as factors.

Source	Type III SS	Df	Mean Squares	F-ratio	p-value
Sites	131.124	2	65.562	89.156	<0.001
Core type	186.677	1	186.677	253.859	<0.001
Site * Core type	13.441	2	6.721	9.139	0.015
Error	4.412	6	0.735		

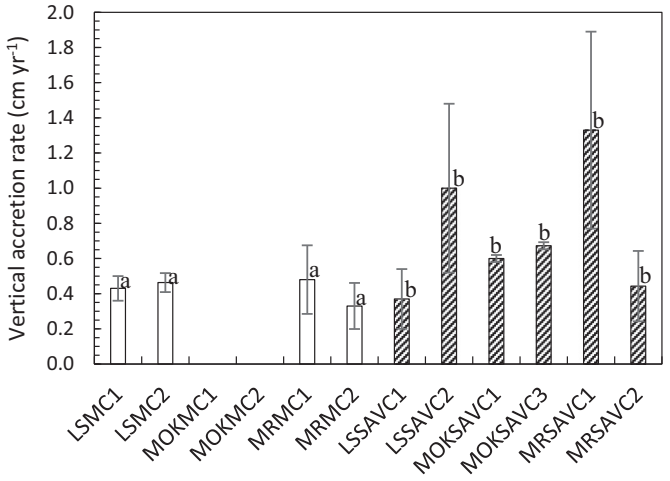

Fig. 6. Estimated vertical accretion rates over the datable period (top ~30 cm) for marsh cores and SAV cores at each of the sites. Core labels are the same as in Fig. 5. MOKMC1 and MOKMC2 could not be dated so no rates could be determined. Different letters (a vs. b) show statistically significant differences between SAV and marsh cores at $p < 0.05$. Error bars represent propagated dating uncertainty (±) as described in methods.

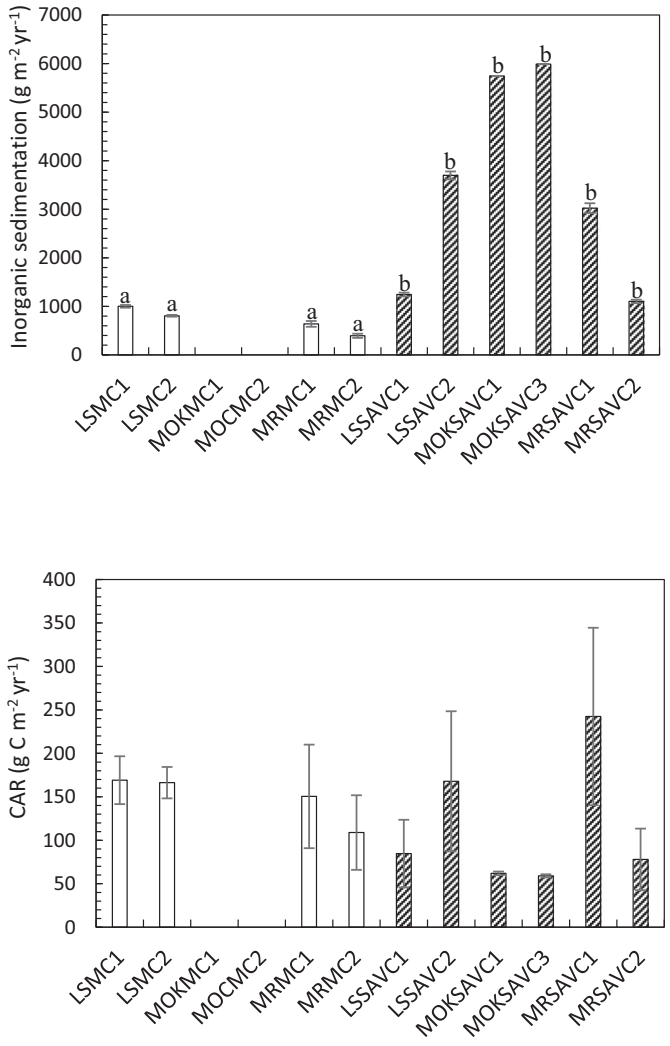

Fig. 7. Mean inorganic sedimentation rate and mean CARs over the datable period (top ~30 cm) for marsh cores (MC) and SAV cores (SAVC) at LS, MR, and MOK. Different letters (a vs. b) show statistically significant differences between SAV and marsh cores at $p < 0.05$. Error bars represent propagated dating uncertainty (±) as described in methods.

for organic carbon and inorganic sediment (Fig. 7). Patches of *E. densa* in the landscape represent distinct environments that differ from both unvegetated channel sediments and marshes in several ways. The top cm of sediments under *E. densa* patches contain lower mean bulk density and higher % organic carbon than adjacent unvegetated channel bed sediments, demonstrating that *E. densa* alters sedimentation within a patch. In comparison to nearby tidal freshwater marshes, sediments under *E. densa* patches have higher bulk density and lower % organic carbon (Fig. 5). This is not surprising as suspended sediment is more readily available to subtidal SAV patches vs. intertidal marshes, while organic matter, and therefore % organic carbon, is much more plentiful in marshes (particularly high productivity bulrush marshes, Byrd et al., 2018, 2020) than SAV patches. In addition, *E. densa* patches have inorganic sedimentation rates (*E. densa*: 1103–5989 g m^{-2} yr^{-1}, marsh: 393–1001 g m^{-2} yr^{-1}, Fig. 7) and vertical accretion rates (*E. densa*: 0.4–1.3 cm yr^{-1}, marsh: 0.3–0.5 cm yr^{-1}, Fig. 6) that are greater than adjacent marshes, but CARs that are quite similar to marshes (*E. densa*: 59–242 g C m^{-2} yr^{-1}, marsh: 109–169 g C m^{-2} yr^{-1}, Fig. 7). The vertical accretion rates, CARs, and inorganic sedimentation rates determined for *E. densa* patches are likely even greater than these estimates because the top 30 cm layer in the cores, which was needed to obtain accurate dating, was likewise used for rate calculations. This layer represents ~23–91 years of deposition, which is longer than the period since widespread *E. densa* infestation began in ~1990 in all cores except LSSAVC2 and MRSAV1 (Supplementary Information: Table A4).

The magnitude and spatial scale of carbon and sediment storage currently found in *E. densa* is likely a new phenomenon in the Delta for several reasons. First of all, none of the other common SAV species found in the Delta are as widely distributed as *E. densa*, which represents up to 66% of SAV cover in the Delta (Santos et al., 2011). This is because *E. densa* can outcompete native SAV in freshwater ecosystems (Hussner and Lösch, 2005; Borgnis and Boyer, 2016) and also because *E. densa* has a heightened capacity to expand its range compared to other species (Santos et al., 2011; Yarrow et al., 2009). Second, two of the other common SAV species in the Delta, *S. pectinata* and *P. nodosus*, have a growth habit that is much less dense than *E. densa*, reducing their ability to produce high amounts of autochthonous carbon and trap sediment from the water column. Third, although *E. canadensis* and *C. demersum*, the two other common species of native SAV in the Delta, do have a dense growth habit, they do not occupy the entire water column. This reduces their ability to trap sediment (Sand-Jensen, 1998; Sand-Jensen and Pedersen, 1999) and so would likely result in lower carbon and sediment storage under these species than *E. densa*. Taken together, these differences in plant traits between native SAV and *E. densa* strongly suggest that, before *E. densa* infestation, freshwater SAV was not as widespread nor as dense in the water column as during post-infestation. Therefore, even though some carbon and sediment storage likely occurs under native freshwater SAV, all these factors strongly suggest that the spatial scale and magnitude of carbon accumulation under *E. densa* is much greater than it would have been prior to infestation in the Delta.

The amount of carbon and sediment stored under *E. densa* is large enough to have meaningful implications for both carbon and sediment budgets in the region. *E. densa* stores approximately 3500 ± 2200 metric tons C yr^{-1} in the Delta (see results), which represents 38% of the carbon stored annually in the ~7879 ha of restored marshes in the Delta region (Drexler et al., 2019). Although this represents just a tiny fraction (<0.004%) of the ~83–100 Tg of carbon lost since mass conversion of the Delta to agriculture (Drexler et al., 2019), it shows that carbon stored in *E. densa* represents a meaningful component of recent blue carbon storage in the Delta. With regard to inorganic sediment, the total amount stored in *E. densa* in the Delta is approximately 103,000 ± 22,000 metric tons yr^{-1} (see results). This sediment sink represents 6.2% of the ~1,660,000 metric tons yr^{-1} of sediment supplied to the Delta from its two major rivers, the Sacramento and San Joaquin,

and 9.4% of the ~1,096,000 metric tons retained in the Delta each year (Schoellhamer et al., 2012; Wright and Schoellhamer, 2005).

Although modest, this sink of inorganic sediment stored in *E. densa* may have implications for marsh formation in the Delta and further downstream in other parts of the San Francisco Estuary. Because most tidal marshes are highly dependent on influxes of inorganic sediment to keep pace with sea-level rise (Kirwan and Megonigal, 2013; Turner et al., 2000), any reduction in sediment availability may jeopardize the ability of marshes to maintain their position in the tidal frame. In the Delta, invasive SAV dominated by *E. densa* lines the channels adjacent to marshes. This physical adjacency is likely causing sediment to be blocked from depositing on the marsh plain, except under spring tide conditions or major storms, when the height of the water column is greater than the height of the *E. densa* canopy. In addition, over the past ~60 years, suspended sediment concentrations in the Delta have been decreasing by ~1.8% per year (Work et al., 2020). Taken together, these factors are likely reducing the resilience of marshes in the Delta and further downstream, which rely on riverine flows for sediment inputs.

The ability of *E. densa* to serve as both a carbon and inorganic sediment sink is controlled to a large extent by hydrodynamics. Our data show that % mud (silt and clay fractions <63 μm) in *E. densa* patches is higher than in the unvegetated channel, indicating preferential trapping of fine sediments in patches where current speeds are lower (Fig. 4). A comparison of our sites shows that a greater proportion of carbon is stored under the lower energy conditions found in LS and MR than at MOK, which is a high energy, mainstem site (Figs. 5, 7). The stronger currents characteristic of MOK resuspend more sediments with a wider range of particle sizes, including coarser particles. As a result, *E. densa* patches at MOK have a higher inorganic sedimentation rate than the other two sites, and the trapped sediment has a lower proportion of fine sediments (% mud) (Figs. 4 and 7). In contrast, the slower currents at LS and MR have less energy to resuspend particles, leading to a greater proportion of fine sediments in *E. densa* patches (Fig. 4) and thus creating the conditions highly conducive to storage of organic matter (Kleeberg et al., 2010; Sand-Jensen, 1998) (Figs. 4 and 7).

In addition to hydrodynamics, several other site-specific factors control the retention of carbon and sediment in SAV. Both carbon and inorganic sediment accumulate in patches of *E. densa* because of the particularly powerful ecosystem engineering capabilities of this species. *E. densa* has a dense growth habit due to its whorled leaves and multiple branches that extend throughout the water column. Such abundant growth of SAV results in a thick canopy throughout the water column, which is highly effective in decreasing water velocity and bed shear stress and leads to deposition of suspended material with little loss from resuspension (Durand et al., 2016; Getsinger and Dillon, 1984; Hestir et al., 2016; Jones et al., 2012; Lacy and Wyllie-Echeverria, 2011; Nepf, 2012; Sand-Jensen, 1998). Submergence depth of the canopy (the ratio of water depth to canopy height) and patch morphology are also key factors determining trapping potential of SAV such as *E. densa* (Liu and Nepf, 2016; Luhar and Nepf, 2013; Nepf and Nepf and Vivoni, 2000). These factors result in a positive feedback hypothesized by Hestir et al. (2016) wherein the bigger and/or denser the patch of *E. densa*, the more water velocity is impeded and the more sediment is trapped in the patch.

The supply of carbon and inorganic sediment also has strong bearing on what can ultimately be trapped in a patch of *E. densa*. The accumulation of autochthonous carbon depends on the balance between primary productivity vs. decomposition and loss. The total availability of carbon depends on both autochthonous and allochthonous sources, which are a function of the diversity and productivity in the greater estuary (Odum, 1980; Valiela et al., 2000). Although data are not available, if *E. densa* is similar at all to seagrasses in carbon trapping, then the allochthonous carbon contribution represents a substantial (up to 50% or more) component of the total sediment carbon sink (e.g., Kennedy et al., 2010).

With regard to inorganic sediment, the supply of material is largely controlled by local suspended sediment concentration, which depends on sediment supply, erodible sediment, and local hydrodynamics (Schoellhamer, 2011). In the Delta, suspended sediment concentration is influenced both by climate and resuspension (Morgan-King and Schoellhamer, 2013; Wright and Schoellhamer, 2005). High flow events in winter and spring import large quantities of sediment and elevate suspended sediment concentrations throughout the system. Resuspension driven by tidal currents increases in importance with distance down estuary. Among our sites, MOK is most subject to high flow events in which currents are strong and SSC is high. These conditions create high potential for sediment trapping in *E. densa* (Fig. 7), but may also wash away material deposited in a patch (Gurbisz et al., 2016). LS and MR are further down estuary, and thus are more tidally dominated. The greater percentage of mud in the channel at these sites (Fig. 4) indicates that most of the sand fraction has settled out further up estuary, and that pulses of sediment supply during high flow events are less important than at MOK.

Our results strongly suggest that significant rates of carbon accumulation are occurring around the world in patches of *E. densa* as well as other invasive SAV with a similar structure such as *Hydrilla verticillata* (GISD, 2009a). This conclusion is supported by the fact that carbon accumulation at our sites occurred across a range of hydrodynamic conditions with highest rates at the two lower energy sites, MR and LS (Fig. 6). Freshwater SAV such as *E. densa* and *H. verticillata* are most typically found in slow flowing, low energy sites, including streams, lakes, and ponds (Cook and Urmi-König, 1984; GISD, 2019a).

Carbon storage in our tidal freshwater *E. densa* sites represents a novel form of blue carbon on the landscape. The mean CAR in *E. densa* at our sites (116 ± 75 g C m^{-2} yr^{-1}) is only slightly less than the mean global rate for seagrasses (120 ± 26 g C m^{-2} yr^{-1}, top m; Murray et al. (2011); 138 ± 38 g C m^{-2} yr^{-1}, top 0.5 m; McLeod et al. (2011)) and within the global range of CARs measured in salt marshes, mangroves, and seagrasses, which constitute the three major blue carbon systems (McLeod et al., 2011; Murray et al., 2011). It is important to note, however, that although invasive SAV at our Delta sites stores significant amounts of organic carbon, the net ecosystem carbon balance and sustained-flux global warming potential (i.e., the climate impact;, Keller, 2019; Neubauer and Megonigal, 2015) have yet to be measured for any species of freshwater SAV. It is therefore possible that because our Delta sites are fresh and not saline, methane emissions may partially counteract the carbon storage in *E. densa* patches (Poffenbarger et al., 2011; Ribaudo et al., 2018).

The ability of *E. densa* to store carbon represents a valuable new ecosystem service in freshwater habitats; however, this newfound capability of *E. densa* does not reduce or offset its numerous, negative ecosystem engineering traits. Although research has shown some inadvertent benefits of non-native, invasive species in their naturalized settings (e.g., Schlaepfer et al., 2010), it is critical, in evaluating the effects of invasive species, to consider the full balance of their positive and negative effects (Vitule et al., 2012). For this reason, planting *E. densa* outside its native range to achieve carbon sequestration benefits would likely result in a disproportionate amount of negative impacts vs. positive gains. However, in areas where *E. densa* infestation is already broadly distributed, its ability to store carbon should be taken into account when considering management actions as it may provide a meaningful contribution to regional carbon storage. Full eradication of *E. densa* is generally not possible in large regions such as the Delta due to the extent of infestation, the high costs of herbicide treatment, and the incomplete efficacy of treatment (Caudill et al., 2019; Curt et al., 2010; Parsons et al., 2007; Parsons et al., 2009; Santos et al., 2009). Therefore, focusing herbicide treatment of *E. densa* on areas needed for navigation and habitat for sensitive flora and fauna would leave other invaded areas to function as a carbon sink.

5. Conclusions

In this paper, we quantified the impact of *E. densa*, an aquatic ecosystem engineer, on sedimentation processes in a large tidal freshwater region. In so doing, we discovered its ability to serve as a long-term sink for blue carbon and inorganic sediment on the landscape. Carbon accumulation rates in *E. densa* patches are similar to adjacent tidal freshwater marshes and within the ranges of blue carbon systems worldwide. Storage of inorganic sediment by *E. densa* is likely reducing marsh resilience by decreasing the amount of sediment available for marsh-building. Our results demonstrate that chronic plant invasions can simultaneously impact biogeochemical cycling and sediment dynamics in freshwater ecosystems. The key to deciphering such changes is to measure processes that occur on scales of decades or longer. The implications of these new ecosystem engineering properties of *E. densa* are likely far-reaching because this species of invasive SAV is found on all continents except Antarctica. Overall, this study demonstrates that the chronic impacts of invasive species cannot be determined without process-level studies on an ecosystem scale.

Supplementary data to this article can be found online at https://doi.org/10.1016/j.scitotenv.2020.142602.

CRediT authorship contribution statement

Judith Z. Drexler: Project administration, Conceptualization, Funding acquisition, Methodology, Formal analysis, Writing - original draft, Data curation. **Shruti Khanna:** Methodology, Writing - review & editing, Funding acquisition. **Jessica R. Lacy:** Formal analysis, Writing - review & editing, Funding acquisition.

Declaration of competing interest

The authors declare that they have no known competing financial interests or personal relationships that could have appeared to influence the work reported in this paper.

Acknowledgements

This project was funded by the US Geological Survey Priority Ecosystems Science Program, which is supported by the Ecosystems Mission Area and, is led by Mike Chotkowski in the San Francisco Bay and Delta. We thank Christopher Fuller for carrying out the radioisotope analyses; John Ward, Jim Orlando, Dan Powers, and Cordell Johnson for their assistance with coring; Curtis Hagen for help with airboat access; and Angela Tan for conducting sediment carbon analyses. We are grateful to David Schoellhamer, Erin Hestir, Jan Vymazal, and the anonymous reviewer for their thoughtful reviews of the manuscript. All push core data used in this paper are in Table A1 of the Supplementary Information and on USGS ScienceBase. All marsh and SAV core data are found in Tables A2–A4 of the Supplementary Information, the USGS National Water Information System (U.S. Geological Survey, 2020), and in Drexler (2020) in USGS ScienceBase. Any use of trade, firm, or product names is for descriptive purposes only and does not imply endorsement by the US Government.

References

Adame, M.F., Neil, D., Wright, S.F., Lovelock, C.E., 2010. Sedimentation within and among mangrove forests along a gradient of geomorphological settings. Estuar. Coast. Shelf Sci. 86, 21–30. https://doi.org/10.1016/j.ecss.2009.10.013.

Ahearn, D.S., Sheibley, R.W., Dahgren, R.A., 2005. Effects of river regulation on water quality in the lower Mokelumne River, California. River Res. Appl. 21, 651–670. https://doi.org/10.1002/rra.853.

Alfasane, M.D.A., Khondker, M., Islam, M.D.S., Bhuiyan, M.A.H., 2010. *Egeria densa* Planchon (Hydrocharitaceae): a new angiospermic record for Bangladesh. Bangl. J. Plant Taxon. 17 (2), 209–213. https://doi.org/10.3329/bjpt.v17i2.6702.

Appleby, P.G., Oldfield, F., 1983. The assessment of ^{210}Pb data from sites with varying sediment accumulation rates. Hydrobiologia. 103, 29–35. https://doi.org/10.1007/BF00028424.

Atwater, B.F., 1980. Attempts to Correlate Late Quaternary Climatic Records Between San Francisco Bay, the Sacramento-San Joaquin Delta, and the Mokelumne River, California. Ph.D. Dissertation. University of Delaware, Newark, Delaware, USA.

Borgnis, E., Boyer, K.E., 2016. Salinity tolerance and competition drive distributions of native and invasive submerged aquatic vegetation in the upper San Francisco Estuary. Estuaries Coast. 39, 707–717. https://doi.org/10.1007/s12237-015-0033-5.

Boudouresque, C., Meinesz, A., Ribera, M.A., Ballestro, E., 1995. Spread of the green alga *Caulerpa taxifolia* (Caulerpales, Chlorophyta) in the Mediterranean: possible consequences of a major ecological event. Sci. Mar.: Topics in Marine Benthos Ecology 59, 21–29.

Boyer, K., Sutula, M., 2015. Factors controlling submersed and floating macrophytes in the Sacramento-San Joaquin Delta. Southern California Coastal Water Research Project. Technical Report No. 870, Costa Mesa, CA.

Brown, L.R., 2003. Will tidal wetland restoration enhance populations of native fishes? San Franc. Estuary Watershed Sci. 1 (1), 1–42. https://escholarship.org/uc/item/2cp4d8wk.

Byrd, K., Ballanti, L., Thomas, N., Ngugen, D., Holmquist, J.R., Simard, M., Windham-Myers, L., 2018. A remote sensing-based model of tidal marsh aboveground carbon stocks for the conterminous United States. ISPRS J. Photogram. 139, 255–271. https://doi.org/10.1016/j.isprsjprs.2018.03.019.

Byrd, K., Ballanti, L., Thomas, N., Nguyen, D., Holmquist, J.R., Simard, M., Windham-Myers, L., 2020. Corrigendum to "A remote sensing-based model of tidal marsh aboveground carbon stocks for the conterminous United States" [ISPRS J. Photogram. 139 (2018) 255–271]. ISPRS Journal Photogram. 166, 63–67. https://doi.org/10.1016/j.isprsjprs.2020.05.005.

California Department of Water Resources, 1995. Sacramento-San Joaquin Delta Atlas. The Resources Agency, State of California https://www.waterboards.ca.gov/waterrights/water_issues/programs/bay_delta/california_waterfix/exhibits/exhibit3/rdeir_sdeis_comments/RECIRC_2646_ATT%203.pdf.

Caudill, J., Jones, A.R., Anderson, L., Madsen, J.D., Gilbert, P., Shuler, S., Heilman, M.A., 2019. Aquatic plant community restoration following the long-term management of invasive *Egeria densa* with fluridone treatments. Manag. Biol. Invasion. 10, 473–485. https://doi.org/10.3391/mbi.2019.10.3.05.

Champion, P.D., Tanner, C.C., 2000. Seasonality of macrophytes and interaction with flow in a New Zealand lowland stream. Hydrobiologia. 441, 1–12. https://doi.org/10.1023/A:1017517303221.

Cloern, J.E., Knowles, N., Brown, L.R., Cayan, D., Dettinger, M.D., Morgan, T., Schoellhamer, D.H., Stacey, M.T., van der Wegen, M., Wagner, R.W., Jasby, A.D., 2011. Projected evolution of California's San Francisco bay-delta-river system in a century of climate change. PLoS One 6 (9), e24465. https://doi.org/10.1371/journal.pone.0024465.

Conomos, T.J., Smith, R.E., Gartner, J.W., 1985. Environmental setting of San Francisco Bay. Hydrobiologia. 129, 1–12. https://doi.org/10.1007/BF00048684.

Conrad, J.L., Biban, A.J., Weinersmith, K.I., De Carion, D., Young, M.J., Crain, P., Hestir, E.L., Santos, M.J., Sih, A., 2016. Novel species interactions in a highly modified estuary: association of largemouth bass with *Egeria densa*. Trans. Am. Fish. Soc. 145 (2), 249–263. https://doi.org/10.1080/00028487.2015.1114521.

Cook, C.D.K., Urmi-König, K., 1984. A revision of the genus *Egeria* (Hydrocharitaceae). Aquat. Bot. 19 (1–2), 73–96. https://doi.org/10.1016/0304-3770(84)90009-3.

Curt, M.D., Aguado, P.L., Fernández, J., 2010. Proposal for the biological control of *Egeria densa* in small reservoirs: a Spanish case. J. Aquat. Plant Manag. 48, 124–127. https://www.apms.org/japm/vol48/vol48p124.pdf.

Cutshall, N.H., Larsen, I.L., Olsen, C.R., 1983. Direct analysis of ^{210}Pb in sediment samples: self-absorption corrections. Nucl. Instrum. Methods. Phys. 306, 309–312. https://doi.org/10.1016/0167-5087(83)91273-5.

Davidson, I.C., Cott, G.M., Devaney, J., Simkanin, C., 2018. Differential effects of biological invasions on coastal blue carbon: a global review and meta-analysis. Glob. Change Biol. 24, 5218–5230. https://doi.org/10.1111/gcb.14426.

Drexler, J.Z., 2011. Peat formation processes through the millennia in tidal marshes of the Sacramento-San Joaquin Delta, California, USA. Estuaries Coast. 34, 900–911. https://doi.org/10.1007/s12237-011-9393-7.

Drexler, J.Z., 2020. Radioisotopes, percent organic carbon, percent inorganic sediment, and bulk density for peat and sediment cores collected in the Sacramento-San Joaquin Delta, California. U.S. Geological Survey data release https://doi.org/10.5066/P94F5578.

Drexler, J.Z., de Fontaine, C.S., Brown, T.A., 2009. Peat accretion histories during the past 6,000 years in marshes in the Sacramento–San Joaquin Delta, California, USA. Estuaries Coast. 32 (5), 871–892. https://doi.org/10.1007/s12237-009-9202-8.

Drexler, J.Z., Fuller, C.C., Orlando, J., Salas, A., Wurster, F.C., Duberstein, J.A., 2017. Estimation and uncertainty of recent carbon accumulation and vertical accretion in drained and undrained forested peatlands of the southeastern USA. J. Geophys. Res. Biogeosci. 122 (10), 2563–2579. https://doi.org/10.1002/2017JG003950.

Drexler, J.Z., Fuller, C.C., Archfield, S., 2018. The Approaching Obsolescence of ^{137}Cs Dating of Wetland Soils in North America. Quat. Science Rev. https//doi.org/https://doi.org/10.1016/j.quascirev.2018.08.028.

Drexler, J.Z., Khanna, S., Schoellhamer, D.H., Orlando, J., 2019. The fate of blue carbon in the Sacramento-San Joaquin Delta of California, USA. In: Windham-Myers, L., Crooks, S., Troxler, T.G. (Eds.), A Blue Carbon Primer: The State of Coastal Wetland Carbon Science, Practice, and Policy. CRC Press, Taylor Francis Group, Boca Raton, pp. 307–326.

Durand, J., Fleenor, W., McElreath, R., Santos, M.J, Moyle, P., 2016. Physical controls on the distribution of the submersed aquatic weed *Egeria densa* in the Sacramento–san Joaquin Delta and implications for habitat restoration. San Franc. Estuary Watershed Sci.14(1), 1–20. https://escholarship.org/uc/item/85c9h479.

Evangelista, H.B.A., Thomaz, S.M., Umetsu, C.A., 2014. An analysis of publications on invasive macrophytes in aquatic ecosystems. Aquat. Invasions 9 (4), 521–528. https://doi.org/10.3391/ai.2014.9.4.1.

Gallardo, B., Clavero, M., Sanchez, M.I., Vilá, M., 2016. Global ecological impacts of invasive species in aquatic ecosystems. Glob. Change Biol. 22, 151–163. https://doi.org/10.1111/gcb.13004.

Ganthy, F., Soissons, L., Sauriau, P., Verney, R., Sottolichio, A., 2015. Effects of short flexible seagrass *Zostera noltei* on flow, erosion and deposition processes determined using flume experiments. Sedimentology. 62, 997–1023. https://doi.org/10.1111/sed.12170.

Getsinger, K.D., Dillon, C.R., 1984. Quiescence, growth and senescence of *Egeria densa* in Lake Marion. Aquat. Bot. 20 (3–4), 329–338. https://doi.org/10.1016/0304-3770(84)90096-2.

Gillard, M., Thiebaut, G., Deleu, C., Leroy, B., 2017. Present and future distribution of three aquatic plants taxa across the world: decrease in native and increase in invasive ranges. Biol. Invasions 19 (7), 2159–2170. https://doi.org/10.1007/s10530-017-1428-y.

Global Invasive Species Database, 2019a. Species profile: *Hydrilla verticillata*. http://www.iucngisd.org/gisd/species.php?sc=272/ (accessed 13 December 2019).

Global Invasive Species Database, 2019b. Species profile: *Egeria densa*. http://www.iucngisd.org/gisd/speciesname/Egeria+densa accessed 13 December 2019.

Gurbisz, C., Kemp, W.M., Sanford, L.P., Orth, R.J., 2016. Mechanisms of storm-related loss and resilience in a large submersed plant bed. Estuaries Coast. 39, 951–966. https://doi.org/10.1007/s12237-016-0074-4.

Hargis, T.G., Twilley, R.R., 1994. Improved coring device for measuring soil bulk density in a Louisiana deltaic marsh. J Sediment Res A Sediment Petrol Process. 64 (3a), 681–683. https://doi.org/10.1306/D4267E60-2B26-11D7-8648000102C1865D.

Hatton, R.S., DeLaune, R.D., Patrick Jr., W.H., 1983. Sedimentation, accretion, and subsidence in marshes of Barataria Basin. Louisiana. Limnol. Oceanogr. 28 (3), 494–502. https://doi.org/10.4319/lo.1983.28.3.0494.

Hestir, E.L., Schoellhamer, D.H., Greenberg, J., Morgan-King, T.L., Ustin, S.L., 2016. The effect of submerged aquatic vegetation expansion on a declining turbidity trend in the Sacramento-San Joaquin River Delta. Estuaries Coast. 39 (4), 1100–1112. https://doi.org/10.1007/s12237-015-0055-z.

Hillman, E.R., Rivera-Monroy, V.H., Nyman, J.A., La Peyre, M.K., 2020. Estuarine submerged aquatic vegetation habitat provides organic carbon storage across a shifting landscape. Sci. Total Environ. 717, 137217. https://doi.org/10.1016/j.scitotenv.2020.137217.

Hussner, A., Lösch, R., 2005. Alien aquatic plants in a thermally abnormal river and their assembly to neophyte-dominated macrophyte stands. Limnologica. 35, 18–30. https://doi.org/10.1016/j.limno.2005.01.001.

Jepson Flora Project, 2020. Jepson eFlora. http://ucjeps.berkeley.edu/eflora/ accessed 08 January 2020.

Jones, C.G., Lawton, J.H., Shachak, M., 1994a. Organisms as ecosystem engineers. Oikos 69 (3), 373–386. https://doi.org/10.2307/3545850.

Jones, C.G., Lawton, J.H., Shachak, M., 1994b. Positive and negative effects of organisms as physical ecosystem engineers. Ecology. 78 (7), 1946–1957. https://doi.org/10.1890/0012-9658(1997)078[1946:PANEOO]2.0.CO;2.

Jones, J.I., Collins, A.L., Naden, P.S., Sear, D.A., 2012. The relationship between fine sediment and macrophytes in rivers. River Res. Appl. 28, 1006–1018. https://doi.org/10.1002/rra.1486.

van Katwijk, M.M., Bos, A.R., Hermus, D.C.R., Suykerbuyk, W., 2010. Sediment modification by seagrass beds: modification and sandification induced by plant cover and environmental conditions. Estuar. Coast. Shelf Sci. 89, 175–181. https://doi.org/10.1016/j.ecss.2010.06.008.

Keller, J.K., 2019. Greenhouse gases. In: Windham-Myers, L., Crooks, S., Troxler, T.G. (Eds.), A Blue Carbon Primer: The State of Coastal Wetland Carbon Science, Practice, and Policy. CRC Press, Taylor Francis Group, Boca Raton, pp. 93–106.

Kennedy, J., Beggins, J., Duarte, C.M., Fourqurean, J.W., Holmer, M., Marbá, N., Middelburg, J.J., 2010. Seagrass sediments as global carbon sink: isotopic constraints. Global Biogeochem. Cycles 24 (4), 1–8. https://doi.org/10.1029/2010GB003848.

Khanna, S., Santos, M.J., Boyer, J.D., Shapiro, K.D., Bellvert, J., Ustin, S.L., 2018. Water primrose invasion changes successional pathways in an estuarine ecosystem. Ecosphere. https://doi.org/10.1002/ecs2.2418.

Kirwan, M.L., Megonigal, J.P., 2013. Tidal wetland stability in the face of human impacts and sea-level rise. Nature. 504, 53–60. https://doi.org/10.1038/nature12856.

Kleeberg, A., Köhler, J., Sukhodolova, T., Sukhokolov, A., 2010. Effects of aquatic macrophytes on organic matter deposition, resuspension and phosphorus entrainment in a lowland river. Freshw. Biol. 55, 326–345. https://doi.org/10.1111/j.1365-2427.2009.02277.x.

Knowles, N., 2002. Natural and management influences on freshwater inflows and salinity in the San Francisco Estuary at monthly to interannual scales. Water Resour. Res. 38, 1289–1299. https://doi.org/10.1029/2001WR000360.

Lacy, J.R., Wyllie-Echeverria, S., 2011. The influence of current speed and vegetation density on flow structure in two macrotidal eelgrass canopies. Limnol. Oceanogr.: Fluids Environ. 1 (1), 38–55. https://doi.org/10.1215/21573698-1152489.

Lavery, P.S., Mateo, M.-A., Serrano, O., Rozaimi, M., 2013. Variability in the carbon storage of seagrass habitats and its implications for global estimates of blue carbon ecosystem service. PLoS One 8 (9), e73748. https://doi.org/10.1371/journal.pone.0073748.

Liao, C., Peng, R., Luo, Y., Zhou, X., Wu, X., Fang, C., Chen, J., Li, B., 2008. Altered ecosystem carbon and nitrogen cycles by plant invasion: a meta-analysis. New Phytol. 177 (3), 706–714. https://doi.org/10.1111/j.1469-8137.2007.02290.x.

Light, T., Grosholz, E.D., Moyle, P.B., 2005. Delta ecological survey (phase I): nonindigenous aquatic species in the Sacramento–San Joaquin Delta, a literature review. Final Report for Agreement DCN 1113322J011. Stockton, CA, US Fish and Wildlife Service.

Liu, C., Nepf, H., 2016. Sediment deposition within and around a finite patch of model vegetation over a range of channel velocity. Water Resour. Res. 52, 600–612. https://doi.org/10.1002/2015WR018249.

Lodge, D.M., Stein, R.A., Brown, K.M., Covich, A.P., Bronmark, C., Garvey, J.E., Klosiewski, S.P., 1998. Predicting impact of freshwater exotic species on native biodiversity: challenges in spatial scaling. Austral. Ecology. 23, 53–67. https://doi.org/10.1111/j.1442-9993.1998.tb00705.x.

Luhar, M., Nepf, H.M., 2013. From the blade scale to the reach scale: a characterization of aquatic vegetative drag. Adv. Water Resour. 51, 305–316. https://doi.org/10.1016/j.advwatres.2012.02.002.

Madsen, J.D., Chambers, P.A., James, W.F., Koch, E.W., Westlake, D.F., 2001. The interaction between water movement, sediment dynamics and submersed macrophytes. Hydrobiologia 444, 71–84. http://link.springer.com/article/10.1023/A%3A1017520800568.

Martin, G.D., Coetzee, J.A., Weyl, P.S.R., Parkinson, M.C., Hills, M.P., 2018. Biological control of *Salvinia molesta* in South Africa revisited. Biol. Control 125, 74–80. https://doi.org/10.1016/j.biocontrol.2018.06.011.

Masifwa, W.F., Twongo, T., Denny, P., 2001. The impact of water hyacinth, *Eichhornia crassipes* (Mart) Solms on the abundance and diversity of aquatic macroinvertebrates along the shores of northern Lake Victoria, Uganda. Hydrobiologia 452, 79–88. https://doi.org/10.1023/A:1011923926911.

McLeod, E., Chmura, G.L., Bouillon, S., Salm, R., Björk, M., Duarte, C.M., Lovelock, C.E., Schlesinger, W.H., Silliman, B.R., 2011. A blueprint for blue carbon: toward an improved understanding of the role of vegetated coastal habitats in sequestering CO_2. Front. Ecol. Environ. 9 (10), 552–560. https://doi.org/10.1890/110004.

Moorhouse, T.P., Macdonald, D.W., 2015. Are invasives worse in freshwater than terrestrial ecosystems? WIREs Water 2, 1–8. https://doi.org/10.1002/wat2.1059.

Morgan-King, T.L., Schoellhamer, D.H., 2013. Suspended-sediment flux and retention in a backwater tidal slough complex near the landward boundary of an estuary. Estuaries Coast. 36, 300–318. https://doi.org/10.1007/s12237-012-9574-z.

Murray, B.C., Pendleton, L., Jenkins, W.A., Sifleet, S., 2011. Green Payments for Blue Carbon: Economic Incentives for Protecting Threatened Coastal Habitats. Nicholas Institute for in Environmental Policy Solutions, Duke University, NI Report 11- 04, Durham, North Carolina.

Nellemann, C., Corcoran, E., Duarte, C.M., Valdés, L., De Young, C., Fonseca, L., Grimsditch, G. (Eds.), 2009. Blue Carbon. A rapid response assessment. United Nations Environment Programme 80.

Nepf, H., 2012. Hydrodynamics of vegetated channels. J. Hydraul. Res. 50 (3), 262–279. https://doi.org/10.1080/00221686.2012.696559.

Nepf, H.M., Vivoni, E.R., 2000. Flow structure in depth-limited, vegetated flow. J. Geophys. Res. 105 (C12), 28,547–28,557. https://doi.org/10.1029/2000JC900145.

Neubauer, S.C., Megonigal, J.P., 2015. Moving beyond global warming potentials to quantify the climate role of ecosystems. Ecosystems. 18, 1000–1013. https://doi.org/10.1007/s10021-019-00422-5.

Nobriga, M.L., Feyrer, F., 2007. Shallow-water piscivore prey dynamics in California's Sacramento–san Joaquin Delta. San Franc. Estuary Watershed Sci. 5 (2), 1–14. http://repositories.cdlib.org/jmie/sfews/vol5/iss2/art4.

Odum, E.P., 1980. The status of three ecosystem-level hypotheses regarding salt marsh estuaries: tidal subsidy, outwelling and detritus-based food chains. In: Kennedy, V.S. (Ed.), Estuarine Perspectives. Academic Press, Cambridge, pp. 485–495.

Parsons, J.K., Hamel, K.S., Wierenga, R., 2007. The impact of diquat on macrophytes and water quality in Battle Ground Lake, Washington. J. Aquat. Plant Manage. 45, 35–39. https://www.apms.org/japm/vol45/v45p35.pdf.

Parsons, J.K., Couto, A., Hamel, K.S., Marx, G.E., 2009. Effect of fluridone on macrophytes and fish in a coastal Washington lake. Aquat. Plant Manage. 47, 31–40. https://media.digitalarchives.wa.gov/do/511ABFFF7DB885CDAF6C4F77A7F23497.pdf.

Poffenbarger, H.J., Needelman, B.A., Megonigal, J.P., 2011. Salinity influence on methane emissions from tidal marshes. Wetlands. 31 (5), 831–842. https://doi.org/10.1007/s13157-011-0197-0.

Powell, K.I., Chase, J.M., Knight, T.M., 2011. A synthesis of plant invasion effects on biodiversity across spatial scales. Am. J. Bot. 98 (3), 539–548. https://openscholarship.wustl.edu/bio_facpubs/19.

Prokopovich, N.P., 1985. Subsidence of peat in California and Florida. Bull. Assoc. Eng. Geol. 22, 395–420. https://doi.org/10.2113/gseegeosci.xxii.4.395.

Reid, A.J., Carlson, A.K., Creed, I.F., Eliason, E.J., Gell, P.A., Johnson, P.T.J., ... Cooke, S.J., 2019. Emerging threats and persistent conservation challenges for freshwater diversity. Biol. Rev. 94, 849–873. https://doi.org/10.1111/brv.12480.

Ribaudo, C., Bertrin, V., Dutartre, A., 2014. Dissolved gas and nutrient dynamics within an *Egeria densa* Planch. Bed. Bot. Lett. 161 (3), 233–241. https://doi.org/10.1080/12538078.2014.932703.

Ribaudo, C., Tison-Rosebery, J., Buquet, D., Gwilherm, J., Jamoneau, A., Abril, G., Anschutz, P., Bertrin, V., 2018. Invasive aquatic plants as ecosystem engineers in an oligo-mesotrophic shallow lake. Front. Plant Sci. 9, 1781. https://doi.org/10.3389/fpls.2018.01781.

Sand-Jensen, K., 1998. Influence of submerged macrophytes on sediment composition and near-bed flow in lowland streams. Freshw. Biol. 39, 663–679. https://doi.org/10.1046/j.1365-2427.1998.00316.x.

Sand-Jensen, K., Pedersen, O., 1999. Velocity gradients and turbulence around macrophyte stands in streams. Freshw. Biol. 42, 315–328. https://doi.org/10.1046/j.1365-2427.1999.444495.x.

Santos, M.J., Khanna, S., Hestir, E.L., Andrew, M.E., Rajapakse, S.S., Greenberg, J.A., ... Ustin, S.L., 2009. Use of hyperspectral remote sensing to evaluate efficacy of aquatic plant management in the Sacramento-San Joaquin River Delta, California. Invasive Plant Sci. Manag. 2 (3), 216–229. https://doi.org/10.1614/IPSM-08-115.1.

Santos, M.J., Anderson, L.W., Ustin, S.L., 2011. Effects of invasive species on plant communities: an example using submersed aquatic plants at the regional scale. Biol. Invasions 13 (2), 443–457. https://doi.org/10.1007/s10530-010-9840-6.

Santos, M.J., Hestir, E.L., Khanna, S., Ustin, S.L., 2012. Image spectroscopy and stable isotopes elucidate functional dissimilarity between native and nonnative plant species

in the aquatic environment. New Phytol. 193 (3), 683–695. https://doi.org/10.1111/j.1469-8137.2011.03955.x.
Schlaepfer, M.A., Sax, D.F., Olden, J.D., 2010. The potential conservation value of non-native species. Conserv. Biol. 25 (3), 428–437. https://doi.org/10.1111/j.1523-1739.2010.01646.x.
Schoellhamer, D.H., 2011. Sudden clearing of estuarine waters upon crossing the threshold form transport to supply regulation of sediment transport as an erodible sediment pool is depleted: San Francisco Bay, 1999. Estuaries Coast. 34, 885–899. https://doi.org/10.1007/s12237-011-9382-x.
Schoellhamer, D., Wright, S., Drexler, J.Z., 2012. A conceptual model of sedimentation in the Sacramento–San Joaquin Delta. San Franc. Estuary Watershed Sci 10 (3), 1–25. https://escholarship.org/uc/item/2652z8sq.
Shlemon, R.J., Begg, E.L., 1975. Late quaternary evolution of the Sacramento–San Joaquin Delta, California. In: Suggate, R.P., Creswell, M.M. (Eds.), Quaternary Studies. The Royal Society of New Zealand, Wellington, pp. 259–266.
Simenstad, C., Toft, J., Higgins, H., Cordell, J., Orr, M., Williams, P., ... Reed, D., 1999. Preliminary results from the Sacramento-San Joaquin Delta breached levee wetland study (BREACH). IEP Newsletter. 12, 15–20. https://pdfs.semanticscholar.org/1c88/6104fd7778dc914a6b2f4a1c06e3d7b95c54.pdf.
Strange, E.F., Hill, J.M., Coetzee, J.A., 2018. Evidence for a new regime shift between floating and submerged invasive plant dominance in South Africa. Hydrobiologia. 817, 349–362. https://doi.org/10.1007/s10750-018-3506-2.
Thompson, J., 1957. The Settlement Geography of the Sacramento-San Joaquin Delta, California. Ph.D. Dissertation. Stanford University, Stanford, CA.
Turner, R.E., Swenson, E.M., Milan, C.S., 2000. Organic and inorganic contributions to vertical accretion in salt marsh sediments. In: Weinstein, M., Kreeger, D.A. (Eds.), Concepts and Controversies in Tidal Marsh Ecology. Kluwer Academic Publishing, Dordrecht, pp. 583–595.
U.S. Department of Agriculture Agricultural Research Service/California Division of Boating and Waterways, 2012. *Egeria densa* control program. https://search.usa.gov/search?utf8=%E2%9C%93&affiliate=agriculturalresearchservicears&query=Egeria+densa+Control+Program (accessed 09 January 2020).
U.S. Department of Agriculture, Natural Resources Conservation Service, 2020. The PLANTS Database. National Plant Data Team, Greensboro, NC, USA http://plants.usda.gov accessed 08 January 2020.
U.S. Geological Survey, 2019. Nonindigenous Aquatic Species Database. Gainesville, Florida, USA https://nas.er.usgs.gov/taxgroup/plants accessed 12 December 2019.
U.S. Geological Survey, 2020. National Water Information System: U. S. Geological Survey web interface. https://doi.org/10.5066/F7P55KJN (accessed 3 May 2020).
Ustin, S.L., Santos, M.J., Hestir, E.L., Khanna, S., Casas, A., Greenberg, J., 2015. Developing the capacity to monitor climate change impacts in Mediterranean estuaries. Evol. Ecol. Res. 16, 529–550. https://www.evolutionary-ecology.com/abstracts/v16/2914.html.
Ustin, S.L., Khanna, S., Bellvert, J., Boyer, J.D., Shapiro, K., 2016. Impact of Drought on Submerged Aquatic Vegetation (SAV) and Floating Aquatic Vegetation (FAV) Using AVIRIS-NG Airborne Imagery. Report to the California Department of Fish and Wildlife Stockton, CA.
Ustin, S.L., Khanna, S., Lay, M., Shapiro, K., 2019. Enhancement of Delta Smelt (*Hypomesus transpacificus*) habitat through adaptive management of invasive aquatic weeds in the Sacramento-San Joaquin Delta. Agreement Number 201700796. Report to the California Department of Water Resources, Sacramento, CA.
Valiela, I., Cole, M.L., McClelland, J., Hauxwell, J., Cebrain, J., Joye, S.B., 2000. Role of salt marshes as part of coastal landscapes. In: Weinstein, M.P., Kreeger, D.A. (Eds.), Concepts and Controversies in Tidal Marsh Ecology. Kluwer Academic Publishing, Dordrecht, pp. 22–38.
Van Metre, P.C., Fuller, C.C., 2009. Dual-core mass-balance approach for evaluating mercury and 210Pb atmospheric fallout and focusing to lakes. Environ. Sci. Technol. 43 (1), 26–32. https://doi.org/10.1021/es801490c.
Vilá, M., Basnou, C., Pyšek, P., Josefsson, M., Genovesi, P., Gollasch, S., ... DAISIE partners, 2009. How well do we understand the impacts of alien species on ecosystem services? A pan-European, cross-taxa assessment. Front. Ecol. Environ. 8 (3), 135–144. https://doi.org/10.1890/080083.
Vilá, M., Espinar, J.L., Hejda, M., Hulme, P.E., Jarošik, V., Maron, J.L., Pergl, J., Schaffner, U., Sun, Y., Pyšek, P., 2011. Ecological impacts of invasive alien plants: a meta-analysis of their effects on species, communities, and ecosystems. Ecol. Lett. 14 (7), 702–708. https://doi.org/10.1111/j.1461-0248.2011.01628.x.
Vitousek, P.M., D'Antonio, C.M., Loope, L.L., Westbrooks, R., 1996. Biological invasions as global environmental change. Am. Sci. 84 (5), 218–228.
Vitule, J.R.S., Freire, C.A., Vazquez, D.P., Nuñez, M.A., Simberloff, D., 2012. Revisiting the potential conservation value of non-native species. Conserv. Biol. 26 (6), 1153–1155. https://doi.org/10.1111/j. 152317392012.01950.x.
Wilcock, R.J., Champion, P.D., Nagels, J.W., Croker, G.F., 1999. The influence of aquatic macrophytes on the hydraulic and physico-chemical properties of a New Zealand lowland stream. Hydrobiologia. 416, 203–214. https://doi.org/10.1023/A:1003837231848.
Windham-Myers, L., Crooks, S., Troxler, T.G., 2019. Glossary. In: Windham-Myers, L., Crooks, S., Troxler, T.G. (Eds.), A Blue Carbon Primer: the State of Coastal Wetland Carbon Science, Practice, and Policy. CRC Press, Taylor Francis Group, Boca Raton Press, pp. xxv–xxvii.
Work, P.A., Downing-Kunz, M., Drexler, J.Z., 2020. Trapping of suspended sediment by submerged aquatic vegetation in a tidal freshwater region: field observations and long-term trends. Estuar. Coasts https://doi.org/10.1007/s12237-020-00799-w.
Wright, S.A., Schoellhamer, D.A., 2005. Estimating sediment budgets at the interface between rivers and estuaries with application to the Sacramento-San Joaquin Delta. Water Resour. Res. 41, W09428. https://doi.org/10.1029/2004WR003753.
Yarrow, M., Marín, V.H., Finlayson, M., Tironi, A., Delgado, L.E., Fischer, F., 2009. The ecology of *Egeria densa* Planchon (Liliopsida: Alismatales): a wetland ecosystem engineer? Rev. Chil. Hist. Nat. 82, 299–313. https://doi.org/10.4067/S0716-078X2009000200010.
Zimmerman, C.F., Keefe, C.W., Bashe, J., 2007. Determination of carbon and nitrogen in sediments and particulates of estuarine/coastal waters using elemental analysis. U.S. Environmental Protection Agency Method 440.0 http://www.caslab.com/;EPA-Methods/PDF/EPA-Method-440.pdf accessed 14 Sept 2019.